Japan Review, 1997, **8**: 193-208

EVALUATION OF ENVIRONMENT USING ELECTRON SPIN RESONANCE (ESR): MICROSCOPE IMAGES OF GYPSUM ($CaSO_4 \cdot 2H_2O$) MICROCRYSTALS IN BORE-HOLE CORES AT KONYA BASIN, TURKEY

IKEYA, Motoji, OKA, Toshihide and OMURA, Tetsuji

Department of Earth and Space Science, Graduate School of Science, Osaka-University Osaka, Japan

OKAWA, Makio and TAKENO, Setsuo

Department of Earth and Planetary System Science, Faculty of Science, Hiroshima University, Hiroshima, Japan

Some of the natural minerals formed in arid climate give information on the paleo-climate. A microwave spectroscopy of electron spin resonance, (ESR), which detects the concentration of accumulated defects produced by natural radiation, gives the age of a mineral. ESR ages of gypsum ($CaSO_4 \cdot 2H_2O$) from Quaternary lacustrine sediments in Konya Basin, Turkey, were estimated using the CO_3^- signal as a function of the depth. The ages at 17.4 and 27.4 m were estimated to be about 37 and 62 ka and the average velocity of sedimentation from 6 to 13 m and from 17 to 26 m was determined to be about 0.4 m/ka. The distribution of two radicals (CO_3^- and SO_2^-) in crystalline gypsum was imaged using a scanning ESR microscope developed in our laboratory. The high concentration of SO_2^- at the center of the crystal indicates that the gypsum has grown from the center to the surface. The distribution of impurities was also checked by electron probe X-ray microanalysis (EPMA). Our scanning ESR imaging method can clarify the stripe pattern and cyclic variation of paleo-climate.

Key words: ESR DATING, ESR IMAGING, GYPSUM, DEHYDRATION, PALEO-CLIMATE.

INTRODUCTION

The climate changes since the last glacial age in the Konya Basin, Turkey, are of specific interest in relation to the development of civilizations. Sediments of the Konya Basin, have been investigated to clarify the vegetation and climatic history. Boring cores of sediments were obtained and analyzed for pollen, diatoms, dust and volcanic ash (Yasuda *et al.* 1992). In addition, we have measured some minerals in the boring cores using the electron spin resonance (ESR) method to assess the environmental changes, since ESR and ESR microscopy are useful techniques (Ikeya, 1993).

Gypsum ($CaSO_4 \cdot 2H_2O$) is a widespread sulfate mineral which is often formed by precipitation from saline water in arid areas. Gypsum is useful for ESR dating based on the measurements of accumulated defects, because it has unpaired electrons produced by natural radiation after crystallization (Ikeda and Ikeya 1992). Paramagnetic species of impurity-related CO_3^- defects are formed by natural radiation in gypsum. The total dose of natural radiation *(TD)* is obtained using an additive dose method. The age is determined by assessing the annual dose rate in the ESR dating (Ikeya, 1993).

The distribution of defects due to natural radiation effects as well as paramagnetic impurities can now be imaged using a scanning ESR microscope developed in our laboratory (Furusawa and Ikeya 1988, 1990). Fossils of anmonite, crinoid, shark's teeth and dinosaur eggs have been imaged so far but no Quaternary mineral has been imaged due to the low signal to noise ratio (S/N). If the *TD* (or ESR age) and the content of impurities could be determined for each pixel in an ESR image, the distribution of radioactive elements and mineral growth conditions may be obtained from the images. We have investigated the distributions of paramagnetic impurities and defects in a small gypsum crystal taken from a bore-hole core at the Konya Basin, using the ESR microscope.

It is possible to detect, using ESR and ESR microscope, radiation-induced defects which can not be detected with other methods of analysis. Paramagnetic impurities such as transition metal ions (Mn^{2+} and Fe^{3+}) and rare earth ions can be detected using other methods. Hence an electron probe X-ray microanalysis (EPMA) was also used to determine the distribution of metallic impurities in the mineral and to compare it with the images obtained by ESR (Omura and Ikeya 1996). It can be interpretcd from the ESR image of the *TD* obtained for the first time that the surface of crystal is damaged by the external γ-rays.

EXPERIMENT

Localities of Samples

Konya Basin (37 45′13.3″N., 32 43′05.4″E.) is located about 200 km south of Ankara, the capital of Turkey. Fig. 1 shows the geomorphological map of the Konya Basin in Turkey. Yasuda *et al.* (1992) drilled in the southeastern part of Konya city in 1991 and obtained a core of 60.68 m in length. Detailed description of the core and the results of pollen analysis are reported elsewhere.

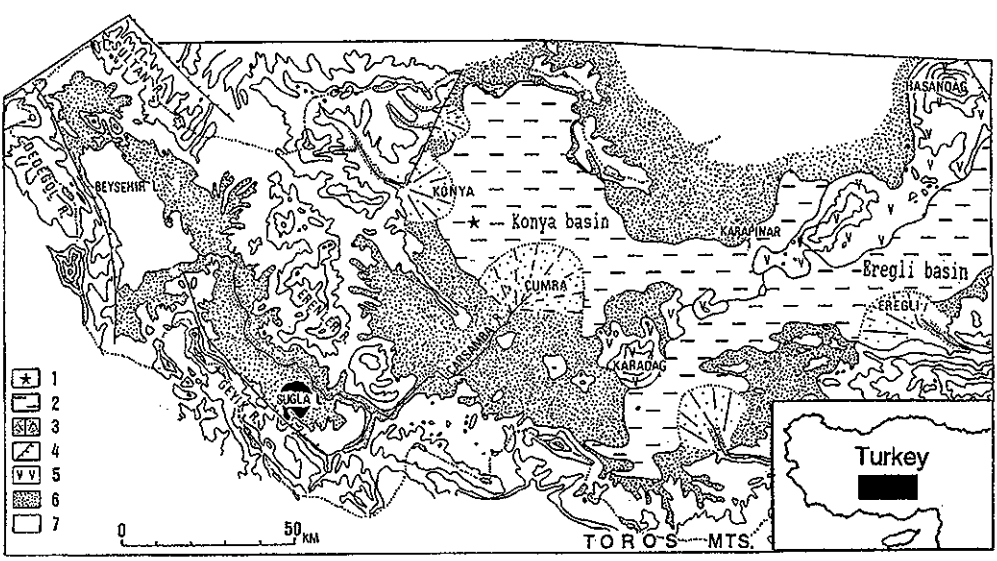

Fig. 1. Geomorphological map of Konya Basin, Turkey partially modified after Fig. 1 in Yasuda *et al.* 1992. 1:Boring site 2:Pluvial lake surface 3:Alluvial fan 4:Fault 5:Volcano 6:Anatolia surface 7:Mountains.

Sample Preparation

(a) Sample for ESR Dating

Gypsum samples from the bore-hole core were crushed into powder, sieved between 100 and 250 μm in diameter, and rinsed with weak hydrochloric acid (0.1 N) for 15 minutes. Each sample was split into seven aliquots and these aliquots were irradiated with γ -rays from ^{60}Co with doses ranging from 0 to 300 Gy.

(b) Sample for ESR imaging

A large mono-crystalline gypsum piece (10 mm×25 mm×20 mm) obtained from the bore-hole core at the depth of 27 m was used for the ESR imaging. Fig. 2a is a sketch of a broken piece of bore-hole core which contatined the gypsum crystal. The gypsum was found in white - light gray clay. The white-light gray clay layers are vertical to the horizontal light brown clay sediment. The gypsum was cut parallel to the perfect cleavage surface (010) into a slice of 1 mm in thickness (Fig. 2b). "Up, Down, Right, Left" and "Center" are surface and central positions of the obtained gypsum, respectively. The b-axis, which is perpendicular to the cleavage surface, is almost parallel to the white-light gray clay layers.

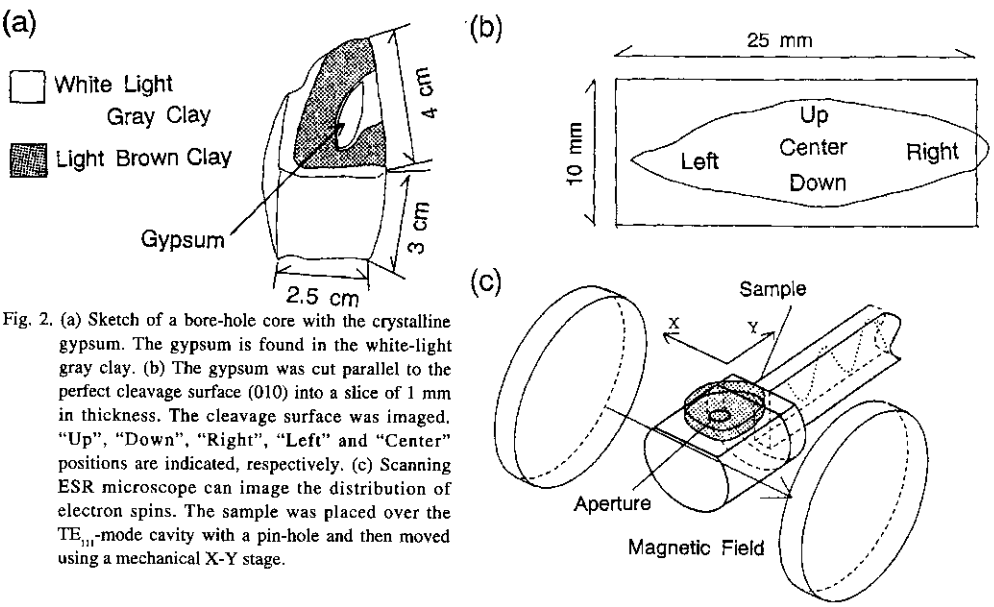

Fig. 2. (a) Sketch of a bore-hole core with the crystalline gypsum. The gypsum is found in the white-light gray clay. (b) The gypsum was cut parallel to the perfect cleavage surface (010) into a slice of 1 mm in thickness. The cleavage surface was imaged. "Up", "Down", "Right", "Left" and "Center" positions are indicated, respectively. (c) Scanning ESR microscope can image the distribution of electron spins. The sample was placed over the TE_{111}-mode cavity with a pin-hole and then moved using a mechanical X-Y stage.

Apparatus

(a) ESR Spectrometer

ESR spectra were measured with a commercial X-band spectrometer (JEOL, RE-1X) at room temperature at 100 kHz field modulation with a modulation amplitude of 0.1 mT and with a microwave power of 20 mW.

(b) ESR microscope

An ESR spectrometer (JEOL, FE-1X) attached to a hand-made cavity and computer-controlled X-Y stage was used as a scanning ESR microscope. The cavity was the TE_{111}-mode cylindrical cavity with an aperture of 3 mm in diameter (Fig. 2c, Furusawa and Ikeya, 1988, 1990). The

cleavage surface of the gypsum was placed over the aperture and was moved after each measurement using a computer controlled X-Y stage. The number of pixels is 1173 (23×51) for the 275 (11×25) mm^2 region.

(c) Radiation assessment

Gamma Ray Spectroscopy

Average ^{238}U, ^{232}Th, ^{40}K concentrations in sediments around the samples were measured by γ-ray spectroscopy using low background spectrometers (GEM-90210 and LOAX-51370/20, Seiko EG&G Ortec) and a hand-made shielding of plastic, pure copper plates and lead blocks from the interior to the outer shielding. Gamma-rays above about 200 keV were carefully measured by GEM-90210 with p-type Ge detector and those below about 200 keV were measured by LOAX-51370/20 with n-type Ge detector.

The sediments were heated at 70°C for 3 days in order to remove water and then placed on the detector. Measurements were made during a period of 2 days and the contents of ^{238}U were calculated from the ^{234}Th, ^{230}Th, ^{226}Ra and ^{214}Pb peaks at 63.3, 67.7, 186.10 and 351.87 keV, respectively. Those of ^{232}Th and ^{40}K were calculated from the ^{228}Ac peak at 911.21 keV and the ^{40}K peak at 1460.83 keV, respectively. The contribution of cosmic rays was tentatively neglected.

Imaging Plate

The distribution of radioactivity (K_2O, U-series) in the gypsum was measured using a commercially available imaging plate (Bas-tⅢ, Fuji Photo Film Co., Ltd) with fine crystals of photo-stimulatable phosphor (BaFBr: Eu^{2+}) in a polyester. When the exposed imaging plate is scanned with a fine laser beam, it emits luminescence proportional to the β-rays dose. This luminescence is collected and imaged.

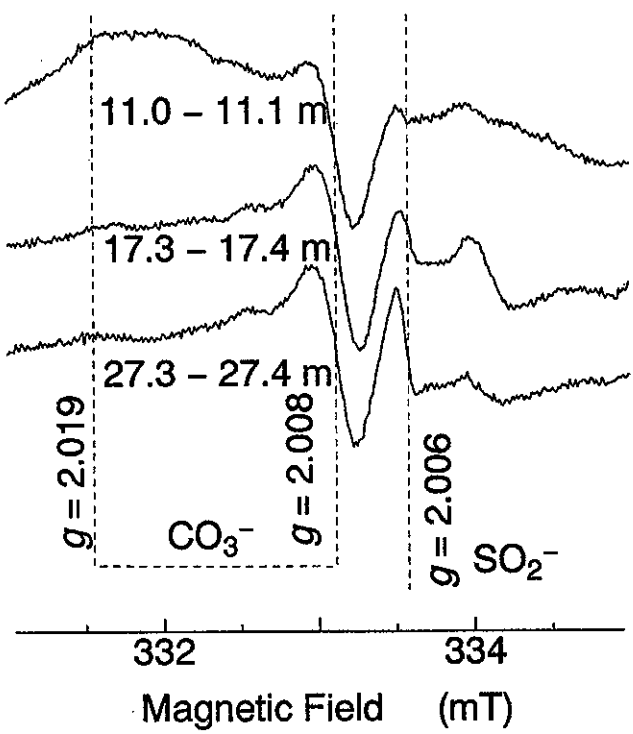

Fig. 3. ESR spectra of gypsum. The signals at $g = 2.006$ and that at $g = 2.019$, $g = 2.008$ were identified as SO_2^- and CO_3^-, respectively.

RESULTS

ESR Spectra of Gypsum

Fig. 3 shows the ESR spectra of gypsum. The signals due to two paramagnetic species were observed at g = 2.006 (SO_2^-), $g_{\parallel}$ = 2.019 and $g_{\perp}$ = 2.008 (CO_3^-) (Ikeya 1993). Other signals that were reported previously in natural gypsum powder could not be observed, presumably because their intensities were large for

relatively young samples or overlapping signals were too complex to be separated (Kasuya *et al.* 1991, Albuquerque and Isotani 1982, Ikeda and Ikeya 1992, Ikeya 1993, Gunter 1967, Wigen and Cowen 1960). Details of ESR signals in gypsum are given in Ikeya (1993).

The Concentration of SO_2^- and CO_3^- with Depth

The concentrations of SO_2^- and CO_3^- in samples are plotted as a function of depth from ground surface in Fig. 4. The concentration of defects are obtained by comparing the ESR intensities of the samples with that of the standard sample, in which the number of defects are known.

Deeper samples show higher concentration of SO_2^-. The concentration of CO_3^- also tends to increase with depth; however there is some reversal for the deepest samples as shown in Fig. 4, because the concentration of CO_3^- depends on the concentration of the impurity CO_3^{2-} as well as the annual dose.

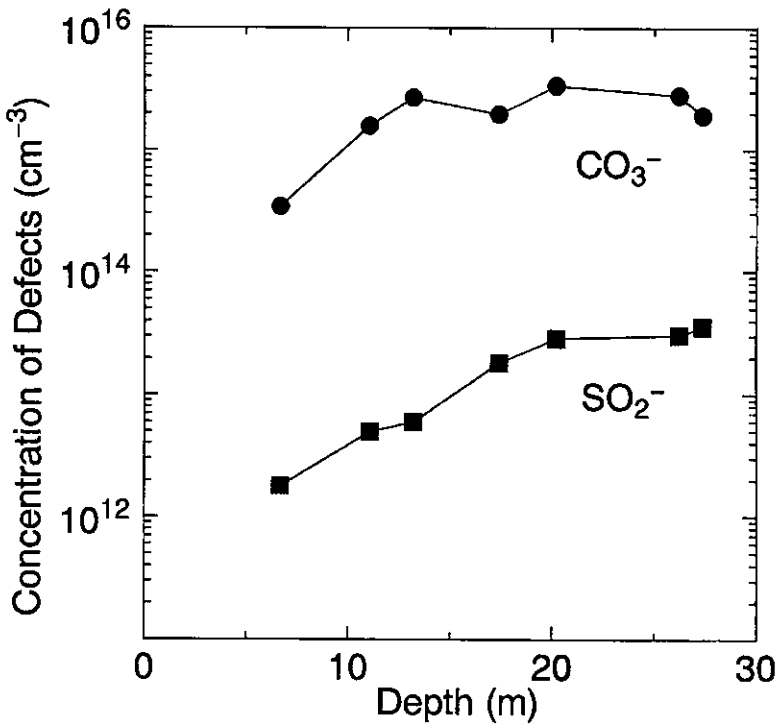

Fig. 4. The concentrations of SO_2^- are higher in the samples at deeper points. But there are some reversal points for those of CO_3^- which depend on the concentration of the impurities as well as the annual dose.

Thermal Annealing of Natural and Irradiated Gypsum

Natural gypsum at 17.3-17.5 m depth and the one irradiated with γ-rays from ^{60}Co with 126 Gy were isochronally (15 minutes duration) heated at several temperatures varying from 70°C to 200°C to investigate the formation and decay of the SO_2^- and CO_3^- defects. The SO_2^- defects were produced by thermal annealing in air as shown in Fig. 5. Two peaks were observed at 120°C and 180°C. The peak at 120°C indicates the loss of 3/2 molecules of water and the peak at 180°C indicates the loss of the remaining water, because gypsum is converted to the semi-hydrate

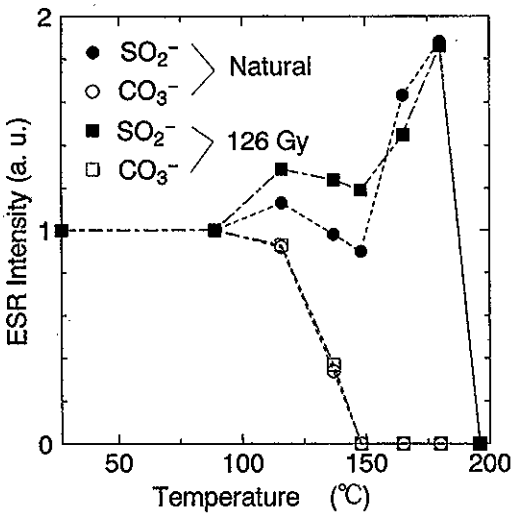

Fig. 5. The enhancement of SO_2^- and decay of CO_3^- were observed by thermal annealing in air. Two peaks of SO_2^- correspond to the loss of water.

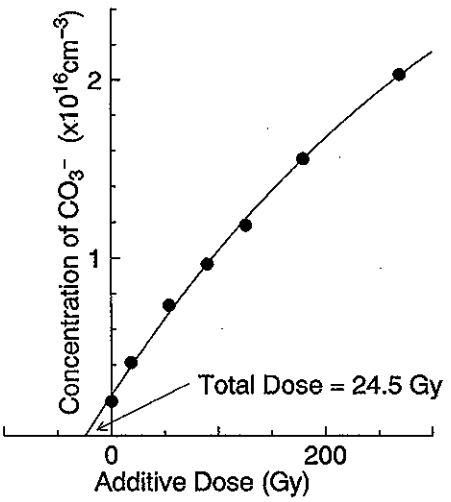

Fig. 6. The growth curve of CO_3^-. The concentration is used for dating.

($CaSO_4 \cdot 1/2H_2O$) and anhydride ($CaSO_4$) at 100~200°C (Deer *et al.* 1966). The SO_2^- defect may be induced by dehydration.

The ESR Dating of Gypsum

Fig. 6 shows the growth curve of CO_3^- in the sample at the depth of 17.3-17.5 m against the additive γ-irradiation. The amplitudes of CO_3^- signal are taken as the signal intensities because CO_3^- is suitable for ESR dating of gypsum (Kasuya *et al.* 1991, Chen *et al.* 1988,1989, Ikeda and Ikeya 1992).

When the lifetime of defects is considered to be infinite, formation and decay of defects in nature are described as

$$dn/dQ = a(1-n/n_s) \quad (1)$$

where the following parameters are used:

n : Concentration of defects [defects/cm^3].

a : Defect creation efficiency [defects/(cm^{3}Gy)].

n_s : Concentration of defect saturated by insensitive volume to radiation [defects/cm^3]

Q : The dose of artificial γ-rays [Gy].

TD : The total dose by natural radiation of the sample after precipitation [Gy].

The solution of Eq.(1) with the boundary condition of $n(\infty) = n_s$ is

$$n = n_s(1-\exp[-a(Q+TD)]) \quad (2)$$

The values of the parameters, a, n_s and TD were determined by extrapolating Eq.(2) to the zero ordinate as shown in Table 1.

The high value of a indicates the high concentration of the impurity CO_3^{2-}, included in gypsum because the CO_3^- defect is considered to be produced from CO_3^{2-}. The saturation concentration corresponds to the ratio of the number of the available lattice sites, N_0, and interaction volume defined as the number of lattice sites insensitive to radiation, b, following Ikeya (1993).

Table 1. The values of the parameters, a, n_s and TD.

Depth (m)	a ($\times 10^{13}$ cm^{-3} Gy^{-1})	n_s ($\times 10^{15}$ cm^{-3})	TD (Gy)
6.6±0.1	3.3±0.3	6.8±0.3	6.8–10.2
11.0±0.1	5.4±0.2	10±1	29–32
13.2±0.1	5.5±1.1	31±5	48–55
17.4±0.1	9.7±2.0	39±6	21–30
20.2±0.1	5.9±1.3	16±2	56–76
26.0±0.1	8.4±1.2	19±2	33–44
27.4±0.1	5.6±0.8	17±2	30–39

$$n_s = N_0/b \tag{3}$$

The TD is related with an ESR age, T, as follows.

$$TD = T \times D \tag{4}$$

The annual dose, D, is determined by estimation of the annual internal dose, D_{IN}, and the annual external dose, D_{EX}, as follows.

$$D = D_{IN} + D_{EX} \tag{5}$$

where D is constant for ^{238}U-series equilibrium. The radiation energies of the radioactive elements and D were used according to the recent papers by Nambi and Aitken 1986, Liritzis and Kokkoris 1992 and Ogoh *et al.* 1993.

The value of D_{IN} was estimated using the gypsum obtained from the core at 26.2 m depth shown in Table 2(a). A defect production efficiency of α-rays relative to that of the artificial irradiation (k) of 0.1 was used. Values of D_{EX} were estimated using the sediments around the samples at each depth as shown in Table 2(b). Values of D_{IN} and D_{EX} were estimated by considering the β-dose attenuation (Mejdahl 1979, Yokoyama *et al.* 1982).

The relation between the ESR ages and the depth are shown in Fig. 7. The extrapolated broken line indicates the relation between the depth and the age derived from the average velocity of sedimentation.

ESR Image

The distribution of the two defects was obtained using a microwave scanning ESR microscope. "Center" position gives a high intensity for SO_2^- produced by chemical reaction (Omura *et al.* 1994) (Fig. 8a). "Up" and "Down" positions give high intensities for CO_3^- produced by natural radiation as shown in Fig. 8b.

Distribution of Total Dose *(TD)*

The ESR images of the gypsum before and after γ-irradiation were obtained in order to investigate the spatial distribution of the total dose as shown in Fig. 9. The total dose by natural radiation, TD, of the sample was determined by extrapolating the growth curve of the signal intensities, I, to zero ordinate. A fitted straight line as a function of dose, Q,

$$I = I_0 (1 + Q/TD)$$

Table 2. (a) The concentration of the radioactive elements in gypsum and the annual dose, D_{IN}.
(b) The concentration of radioactive elements, that of H_2O in sediment around the sample and the annual external dose, D_{EX}.

(a)

	U (ppm)	Th (ppm)	K_2O (%)	D_{IN} (mGy/y)
Gypsum at 26.2m	≦ 0.2	≦ 0.3	≦ 0.02	≦ 0.2

(b)

Depth (m)	U (ppm)	Th (ppm)	K_2O (%)	H_2O (%)	D_{EX} (mGy/y)
6.6±0.1	4.1±0.2	11.5±0.3	2.44±0.04	13.1±0.1	2.03±0.05
11.0±0.1	3.1±0.2	7.8±0.2	1.19±0.02	14.0±0.1	1.37±0.04
13.2±0.1	3.5±0.2	8.8±0.2	1.56±0.03	14.7±0.1	1.85±0.05
17.4±0.1	4.4±0.2	6.8±0.2	1.00±0.02	13.1±0.1	1.36±0.04
20.2±0.1	4.6±0.2	15.3±0.3	2.39±0.04	13.4±0.1	2.86±0.07
26.2±0.1	2.6±0.2	8.7±0.2	1.34±0.03	10.8±0.1	1.13±0.04
27.4±0.1	2.7±0.2	13.8±0.3	1.81±0.03	17.9±0.1	1.30±0.03

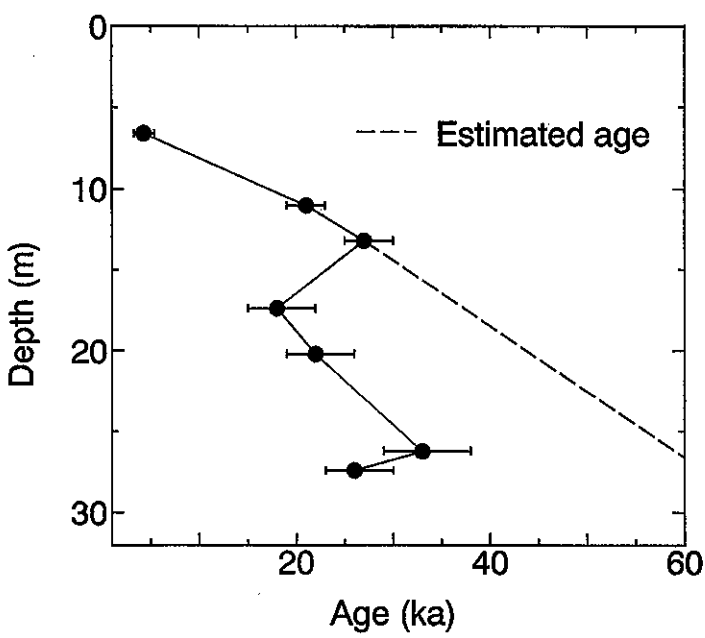

Fig. 7. The relation between the ESR age and depth. The broken line indicates the age derived from the average velocity of sedimentation.

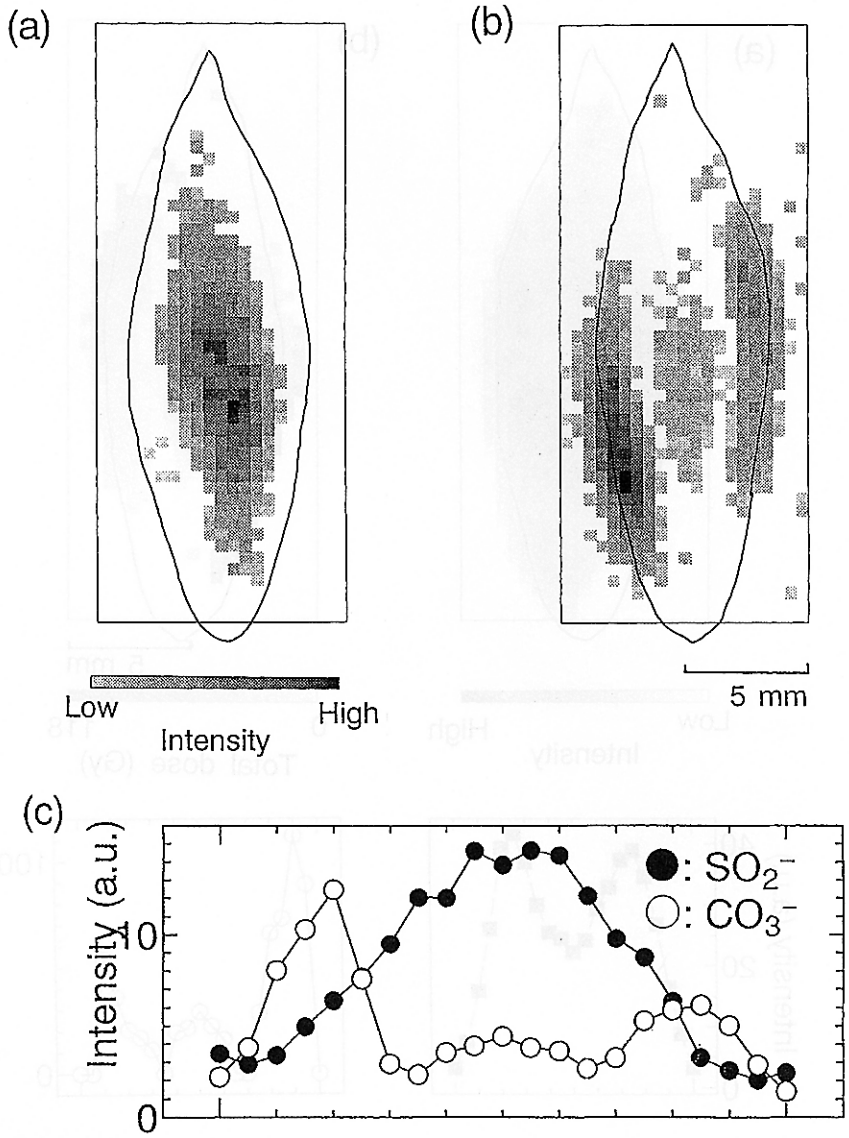

Fig. 8. (a) The distribution of SO_2^-. The central position gave a high intensity.
(b) The distribution of CO_3^-. The surface gave a high intensity.
(c) The distribution of the ESR intensities of SO_2^- and CO_3^- along the central horizontal line in the images.

was used, where I_0 is the initial intensity before additive irradiation. It is considered that the growth is linear in this dose range. The *TD* at "Up" and "Down" surfaces are higher than that at "Center" position either because of heterogeneous distribution of radioactive elements or of the external radiation (Fig. 8b). The *TD* image corresponds to the CO_3^- image.

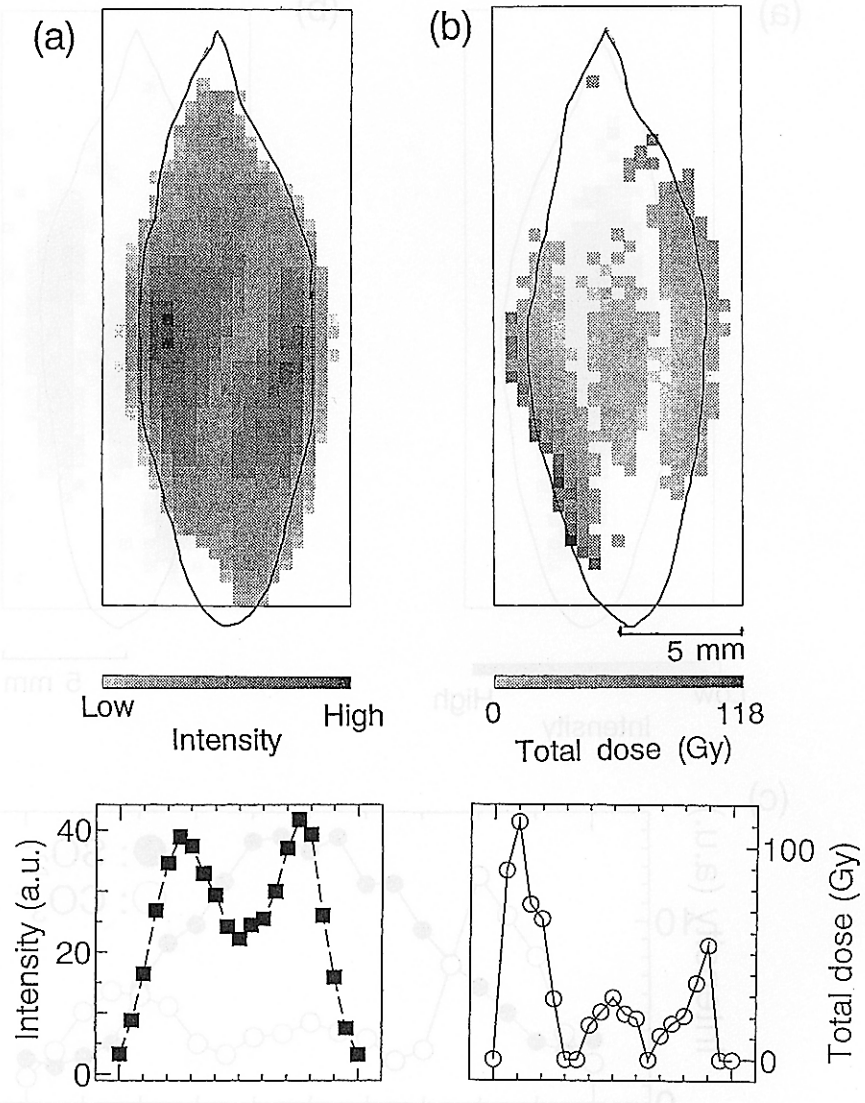

Fig. 9. (a) The image of CO_3^- irradiated up to 118 Gy. The image of *TD* is obtained with this image and Fig. 8(b) by the additive dose method.
(b) The image shows the *TD* of surface is higher. The image corresponds to the CO_3^- image.

Distribution of Impurity, CO_3^{2-}

Distribution of impurity, CO_3^{2-} was determined by irradiating up to the dose of 12 kGy by γ-rays from the source of ^{60}Co much heavier than *TD* (The maximum of *TD* is less than 250 Gy). If the intensity of CO_3^- is in proportion to the concentration of CO_3^{2-}, the distribution of CO_3^{2-} may be obtained as an image of CO_3^- by heavy irradiation (Fig. 10). The obtained image would indicate that the surface ("Up", "Down", "Left" and "Right") has a high concentration of CO_3^{2-}.

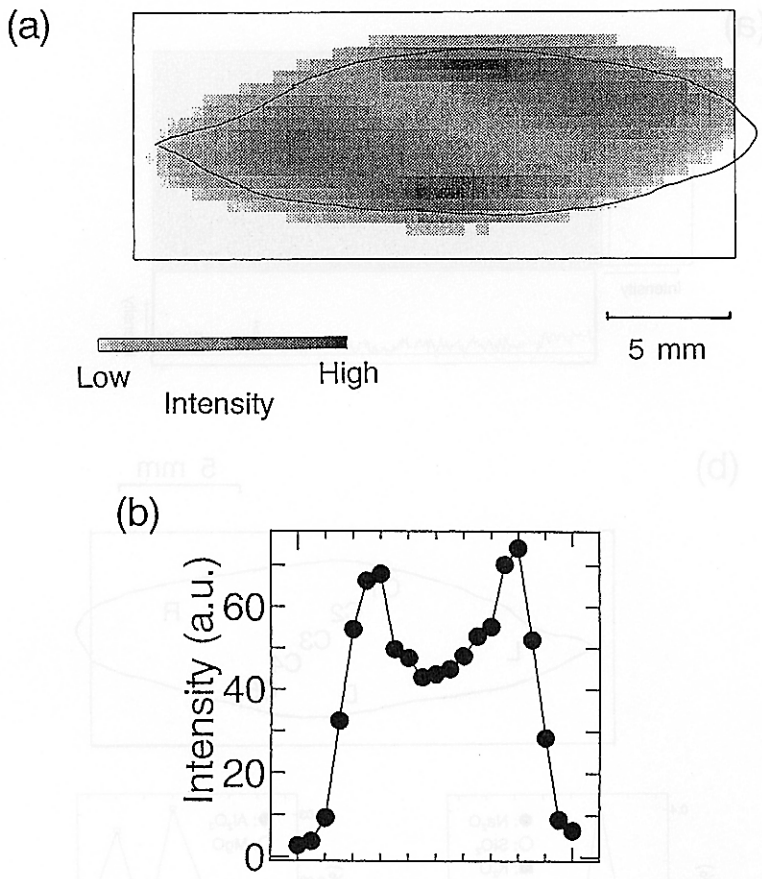

Fig. 10. The distribution of CO_3^{2-} was obtained by heavy irradiation. The local concentration of CO_3^{2-} may be high at that portion which has been crystallized later.

Radioactive Elements Using an Imaging Plate

The imaging plate accumulates and stores the β-rays energy : The coated surface 10 μm in thickness absorbs α-rays. The gypsum had been placed on the imaging plate for 10 days in the shield of lead blocks for radiation exposure. The internal dose rate of β-rays was measured with the imaging plate. The intensity around the gypsum was higher than that in the gypsum, because the dose rate in the air was higher than that in the gypsum. There is no heterogeneous distribution of β emitters within the fluctuation less than 0.1 %. The concentration of K_2O was calibrated by comparing the standard sample of KCl assuming that the source of β-rays was ^{40}K in natural K (Fig. 11a).

Heavy Metal Ions with EPMA

The concentrations of impurities, Na, K, Mg, Al, Si and Fe at eight points of the gypsum were measured with an electron probe X-ray microanalysis (EPMA) (Fig. 11b). Fe at all points were not detectable with EPMA. (The concentration of Fe is less than 0.001 %.) The high intensities of ESR signals, SO_2^-, CO_3^- as well as CO_3^{2-} do not correspond to the concentration of specific

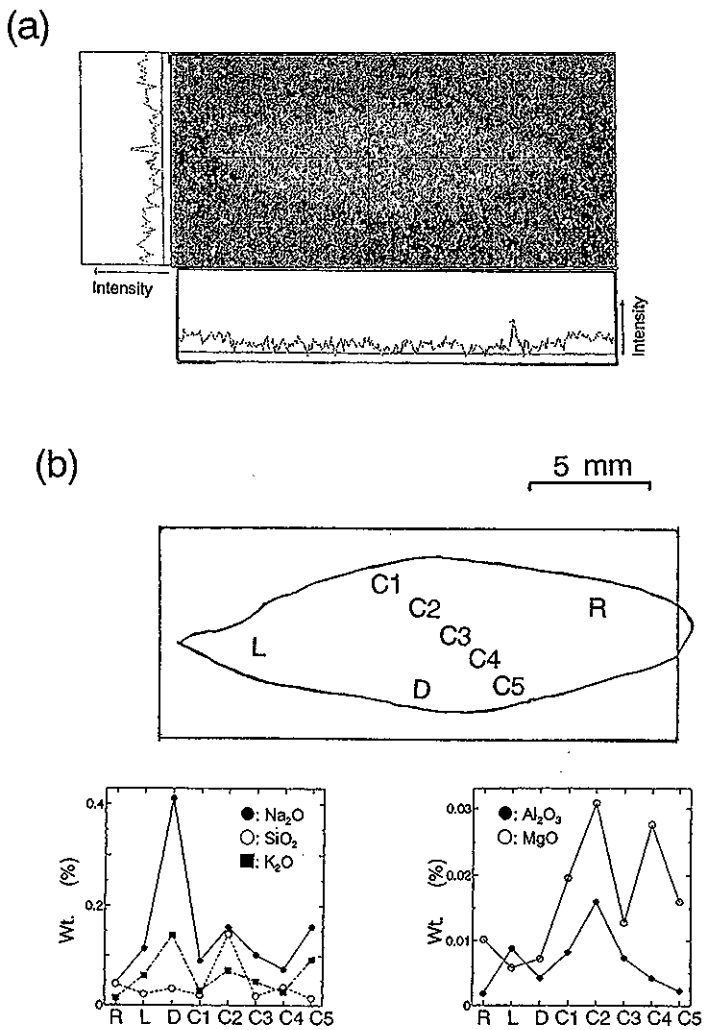

Fig. 11. (a) The distribution of the dose rate from radioactive elements in gypsum was obtained by an imaging plate. There was no hetrogeneous distribution which corresponds to the *TD* image.
(b) The concentrations of impurities, Na, K, Mg, Al, Si and Fe at eight points were measured with EPMA. The concentration of K^+ and Na^+ appear to be higher at D, C5 and C2 where the *TD* and intensity of CO_3^- are high, suggesting the stabilization of a hole (CO_3^-) at monovalent alkali ions. Anomaly of MgO, Al_2O_3 and SiO_2 at C2 may indicate clay mineral inclusion.

metallic impurities detected with EPMA.

DISCUSSION

ESR Age of Gypsum

The ESR ages obtained using the CO_3^- signal were not consistent with the stratigraphy as shown in Fig. 7. The CO_3^- signal was found to decay on dehydration, but the SO_2^- signal was produced by dehydration (see Fig. 5). Gypsum can be converted into anhydrite in pure water at

42°C (Deer *et al.* 1966). The ESR ages would be underestimated because of the decay of CO_3^- caused by repeated dehydration and hydration in nature. Fig. 7 shows that dehydration occured at 17.4 and 27.4 m in the past. The ages at 17.4 and 27.4 m are estimated about 37 and 62 ka respectively according to the average velocity of sedimentation from 6 to 13 m and from 17 to 26 m, 0.408 m/ka. The temperature at 37 and 62 ka before present was lower than that of today according to the variation of paleo-temperature derived from the oxygen isotope ratio (Masuda 1991, Webb et al. 1984). Therefore, the decrease of the CO_3^- might be caused not by a long term variation of climate but by short range events which raised the temperature of sediments at that time. Thus, ESR of radical species in gypsum is a good indicator of the paleo-temperature fluctuation.

Environmental Assessment Using ESR Imaging

(a) Images of SO_2^-

The depth profile of SO_2^- indicates that the intensity of SO_2^- is proportional to the age but it saturates at the age of about 45 ka according to the average velocity of sedimentation (at about 20 m, see Fig. 4 and Fig. 7). SO_2^- produced by chemical reaction indicates growth direction if its intensity is proportional to the age. In the case of gypsum, the image indicates that the gypsum crystallized from the center to the surface. No growth steps were observed under the optical microscope by etching the cleavage surface with water.

(b) Image of CO_3^- induced by natural radiation

The *TD* image indicates that the external β-rays from surrounding sediments would be responsible for the high signal intensity of CO_3^- at the surface for the following reasons (see Fig. 8b and 9b).

1) The distribution of β dose rate indicates homogeneous internal radioactive elements in the crystal (see Fig. 11a).
2) The surface portion having a high *TD* is just about the same range as that of β-rays of 0.5 MeV (1-2 mm) in a solid.

If the external β-rays from surrounding sediments is responsible for the high intensity of signal CO_3^- at the surface, the reasons why only "Up" and "Down" surfaces have high *TD* (see Fig. 8b and 9b) are considered as follows:

1) The crystal has been kept in a crack filled with aqueous solution with the "Up" and "Down" surfaces touched to the sediment as shown in Fig. 12. "Right" and "Left" surfaces would have been exposed to external radiation from radio-active elements in the aqueous solution.
2) "Right" and "Left" surfaces would have recrystallized.

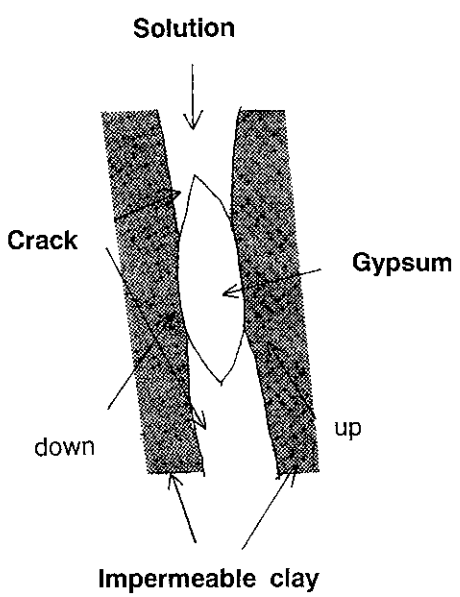

Fig. 12. The gypsum would have been kept in a spread crack with aqueous solution with "Up" and "Down" surface touched to the sediment.

Both reasons imply that the gypsum has been kept in a crack filled with aqueous solution.

(c) Image of CO_3^{2-} as impurities

The image of the CO_3^{2-} concentration would indicate that the CO_3^{2-} concentration at the surface is higher than that at the central position of the gypsum. The variation of CO_3^{2-} in gypsum would be due to the change of CO_3^{2-} in aqueous solution. In a closed system model into sulfate ions precipitate as solid gypsum and CO_3^{2-} ions are repelled solution. Thus, the content of CO_3^{2-} in solution would become higher at the last stage of crystallization. If an open system is established, the variation would correspond to the environmental changes of the aqueous solution at the late stage of crystallization. Further systematic studies of various minerals at the different depths of the bore-core are necessary to clarify the processes of crystallization and the environmental changes.

CONCLUSIONS

ESR dating and imaging of gypsum in bore-hole cores from the Konya Basin were carried out. The ESR ages were obtained using the CO_3^- signal. It was found that the concentration of SO_2^- was larger for deeper samples. The CO_3^- signal decayed on dehydration, but the SO_2^- signal increased on dehydration in a thermal annealing experiment in air. ESR ages may be underestimated because of the decay of CO_3^- by repeated dehydration and hydration of the sediments. The decrease of CO_3^- at 17.4 and 27.4 m might be caused by some short range events which raise the temperature.

The signal intensity of radicals in a sliced crystal of gypsum was imaged with a scanning ESR microscope.

1) The image of SO_2^- concentration indicates the gypsum has grown from the center to the surface.
2) The CO_3^- indicates that the crystalline gypsum has grown in a crack filled with solution in impermeable clay.
3) The distribution of the *TD* indicates that the external β rays from surrounding sediments are responsible for the high intensity of signal CO_3^- at surface.
4) The distribution of CO_3^{2-} was obtained as the CO_3^- image after heavy irradiation. The high concentration of CO_3^{2-} at the last stage indicates either repulsion of CO_3^{2-} ion crystalization or environmental change of aqueous solution.

The ESR microscope would be another useful tool for studying the repulsion of impurities and the ambient environmental changes during mineral growth as well as for imaging radiation effects. From these studies, it is concluded that gypsum precipitated in arid climate about 50 ka.

Acknowledgments

We thank Dr. Y. Yasuda and Dr. Kitagawa at the International Research Center for Japanese Studies for supplying us with gypsum precipitates obtained at the Konya Basin in Turkey and for giving us useful information. We are grateful to Mr. A. Tani and Dr. C. Yamanaka for their help in the experiments and Dr. A. Yoshiasa at Osaka University for valuable suggestions for

analyzing our sample by EPMA. We thank Dr. N. Kimura at the Institute of Industry Science of Osaka University for γ -ray irradiation. This work was supported by a Grant-in-Aid for Scientific Research on Priority Areas (No. 04212116) and also partially by the Priority Area of Earth Evolution Program (No. 259, 1995-1997).

REFERENCES

Albuquerque, A. R. P. L. and Isotani, S. (1982): The EPR Spectra of X-ray Irradiated Gypsum. *J. Phy. Soc. Jpn.*, **51**, 1111-1118.

Chen, Y., Lu, J. Arakel, A. V. and Jacobson, G. (1988): ^{14}C and ESR dating of calcrete and gypcrete cores from the Amadeus Basin, Northern Territory, Australia. *Quaternary. Sci. Rev.*, **7**, 447-453.

Chen, Y., Arakel, A. V. and Lu, J. (1989): Investigation of sensitive signals due to γ -rays irradiation of chemical precipitates. A feasibility study for ESR dating of gypsum, phosphate and calcrete deposits. *Appl. Radiat. Isot.*, **40**, 1163-1170.

Deer, W. A., Howie, R. A. and Zussman, J. (1966): *An Introduction to Rock Forming Minerals.* Longman, Essex, pp. 466-469.

Furusawa, M. and Ikeya, M. (1988): Electron spin resonance imaging of fossil crinoid utilizing localized microwave field. *Anal. Sci.*, **4**, 649-651.

Furusawa, M. and Ikeya, M. (1990): Electron spin resonance imaging utilizing microwave magnetic field. *Jpn. J. Appl. Phys.*, **29**, 270-276.

Gunter, T. E. (1967): Electron paramagnetic resonance studies of the radiolysis of H2O in the solid state. *J. Chem. Phys.*, **6**, 3818-3829.

Ikeda, S. and Ikeya, M. (1992): Electron spin resonance (ESR) signals in natural and synthetic gypsum : An application of ESR to the age estimation of gypsum precipitates from the San Andreas Fault. *Jpn. J. Appl. Phys.*, **31**, 136-138.

Ikeya, M. (1993): *New Applications of Electron Spin Resonance-Dating, Dosimetry and Microscopy-*. World Scientific, Singapore, pp. 211-236.

Kasuya, M. Brumby, S. and Chappell, J. (1991): ESR signals from natural gypsum single crystal: Implications for ESR dating. *Nucl. Tracks Radiat. Meas.*, **18**, 329-333.

Masuda, F. (1991): Evaluation of the present on the history of paleoclimatic change. *J. Geography,* **100**, 976-987 (In Japanese with English abstract).

Mejdahl, V. (1979): Thermoluminescence dating : Beta-dose attenuation in quartz grains. *Archaeometry,* **21**, 61-72.

Nambi, K. S. V. and Aitken, M. J. (1986): Annual dose conversion factors for TL and ESR dating. *Archaeometry,* **28**, 202-205.

Ogoh, K. Ikeda, S. and Ikeya, M. (1993): Confirmation and re-calculation of dose-rate data for TL and ESR dating. *Adv. ESR Appl.*, **9**, 22-28.

Omura, T. Ikeda, S. and Ikeya, M. (1994): ESR dating of gypsum from quaternary lacustrine sediments in Turkey. *Adv. ESR Appl.*, **10**, 14-20.

Webb, T. III (1989): *Global changes of the past,* R. S. Bradley (ed.), UCAR/Office for Interdisciplinary Earth Studies, Boulder, pp. 61-81.

Wigen, P. E. and Cowen, J. A. (1960): Paramagnetic resonance absorption in several electron-

irradiated molecular crystals. *J. Phys. Solids,* **17**, 26-33.
Yasuda, Y. Naruse, T. Kashima, K. Kitagawa, H. and Matsubara, H. (1992): Vegetational and climatic changes since the last glacial age in Turkey and Syria-Especially in relation to the rise and fall of civilizations-. *Environment and Civilization.,* **4**, 13-19.

電子スピン共鳴（ESR）を用いた古環境変遷史の解明
—トルコ・コンヤ盆地のボーリングコア中ジプサム（$CaSO_4 \cdot 2H_2O$）結晶のESR顕微鏡画像—

池谷元伺・岡　俊英・小村哲司・大川真紀雄・竹野節夫

要旨：乾燥した気候のもとで成長した鉱物は過去の気候に関する情報を記録しているものがある。自然放射線によって生成、蓄積される不対電子を検出できる電子スピン共鳴（ESR）は年代測定に利用できる。トルコ・コンヤ盆地の湖成層堆積物からえられた石膏（$CaSO_4 \cdot 2H_2O$）の深さに対してのESR年代値をCO_3^-信号を用いて求めた。深さ17.4mと27.4mにおける年代値は深さ6-13m及び17-26mの区間における平均堆積速度0.4m/kyearから3万7千年、6万2千年となった。2種類のラジカル（CO_3^-及びSO_2^-）の石膏中の分布はESR顕微鏡を用いて得たが、SO_2^-信号は中心部分が強く、この石膏が中心から成長したことを示す結果が得られた。また不純物の分布をEPMAで調べた。